PERGAMON International Journal of Multiphase Flow 25 (1999) 411–432

International Journal of Multiphase Flow

Gas–liquid two-phase flow regimes in rectangular channels with mini/micro gaps

J.L. Xu, P. Cheng, T.S. Zhao *

Department of Mechanical Engineering, Hong Kong University of Science and Technology, Clear Water Bay, Kowloon, Hong Kong

Received 4 November 1997; received in revised form 1 September 1998

Abstract

An adiabatic concurrent vertical two-phase flow of air and water in vertical rectangular channels (12×260 mm) with narrow gaps of 0.3, 0.6–1.0 mm was investigated experimentally. Flow regimes were observed by using a CCD camera and were identified by examining the video images. The flow regimes for gaps of 1.0 and 0.6 mm were found to be similar to those in the existing literature which can be classified into bubbly flow, slug flow, churn–turbulent flow and annular flow. With the decrease of the channel gap, the transition from one flow regime to another occurs at smaller gas flow rates. However, flow regimes for micro-gaps of 0.3 mm or less are quite different from the previous studies: bubbly flow was never observed even at very low gas flow rates. Due to the increased influence of the surface tension force and the frictional shear stress in channels with a micro-gap, the liquid droplets adhered on the wall surface and were pushed by the gas phase. Flow regimes in these micro-gaps can be classified into cap–bubbly flow, slug–droplet flow, churn flow and annular–droplet flow. A previous model has been extended to predict the flow regime transitions from bubbly flow to slug flow, slug flow to churn flow using the bubble rising velocity and the increased frictional coefficient for rectangular channels. A new criterion has been developed to predict the transition of the annular flow. Comparisons of our prediction results with experimental data are discussed for gaps larger than 0.6 mm. With micro-gaps of 0.3 mm or smaller, a new theory needs to be developed.

Keywords: Mini/micro channels; Flow regime; High speed photography; Transition criterion

* Corresponding author. Tel.: 00852 2358 8647; Fax: 00852 2358 1543; e-mail: metzhao@ust.hk.

0301-9322/99/$ - see front matter
PII: S0301-9322(98)00057-3

1. Introduction

To meet the demand of dissipating increasingly larger heat fluxes from electric, power and laser devices, and in compact heat exchangers, attention has been given recently to investigate the flow and heat transfer with or without phase change in micro channels. For example, Peng and Wang (1993), Peng et al. (1995), Peng and Peterson (1996) investigated the flow and heat transfer in micro rectangular channels with water as the working fluid. They measured the single phase frictional pressure drops and heat transfer coefficients, and found that both the pressure drops and heat transfer rate were quite different from the classical correlations. They also studied the sub-cooled boiling heat transfer in micro-channels. Yao and Chang (1983) investigated pool boiling heat transfer in vertical narrow annular with closed bottoms. The boiling heat transfer phenomena was observed through the transparent quartz shroud. With the addition of wall heat flux, the boiling phenomena evolved in the following stages: isolated deformed bubbles, coalesced deformed bubbles, near-dryout and post-dryout conditions and nucleation under slightly deformed bubbles. Bowers and Mudawar (1994) investigated high heat flux boiling in mini-channels and micro-channel heat sinks, and they found that the boiling can dissipate heat fluxes up to 2.0 MW/m^2. Even though there exist a number of studies on convection and boiling of a single component flow in micro-channels, little knowledge has been acquired on multi-component flow and heat transfer in micro/mini channels. Because phase change heat transfer is related to the flow structure, research on two-phase flow patterns in micro/mini channels is necessary in order to understand the phase change heat transfer process. It is this primary need for further analysis of two-phase flow in narrow micro/mini channels that warrants more investigation concerning flow regime pattern identification, transition criteria, void fraction and interfacial concentration.

Early studies of two-phase flow patterns predominantly consisted of flow in circular tubes with diameter $D > 10$ mm. Sadatomi et al. (1982) presented flow regime maps in vertical rectangular channels with hydraulic diameter greater than 10 mm. They clarified flow regimes as bubbly flow, slug flow and annular flow, and indicated that channel geometries have little influence in noncircular channels when the channel hydraulic diameter is larger than 10 mm. Troniewski and Ulbrich (1984) studied 10 different rectangular channels with aspect ratios ranging from 12 to 0.1. Investigations were carried out in vertical channels with aspect ratios in the range of 1 to 12 and in horizontal channels with aspect ratios in the range of 0.1 to 10. The majority of the tests used air/water as the working fluids, and selected tests employed aqueous solutions of sugar/air mixtures in order to study the effect of viscosity. Mishima et al. (1993) used the neutron radiography technique to study the flow in narrow rectangular channels. They measured flow regimes, void fractions, bubble velocity and two-phase pressure drop. They did not find churn flow for gap widths of 1.0 mm. Wilmarth and Ishii (1994) studied adiabatic concurrent and horizontal two-phase flow of air and water through narrow rectangular channels with medium gap widths of 1 and 2 mm. They compared their data with other existing flow regime data. They also compared their experimental data with predictions using Mishima and Ishii (1984) and Taitel et al. (1980) models, and concluded that a new distribution parameter C_o is needed for transition from bubbly flow to slug flow. For the slug to churn flow transition, results were less satisfactory, also due to the distribution model. A

detailed literature review of flow regimes in rectangular channels with a narrow gap is given by Wilmarth and Ishii (1994). Some work has been carried out in this area, but inconsistent conclusions have been made by different authors. Some confusions may come from the flow regime definition and the complicated flow structures themselves.

The present paper is mainly concerned with the flow regime in rectangular channels having a micro/mini gap. Using water and air as the working fluids, flow regimes were determined by carefully examining the video images. Flow regimes for gap widths of 1.0 and 0.6 mm were found to be similar to those in the existing literature, and can be clarified into bubbly flow, slug flow, churn flow and annular flow. But, for gap widths of 0.3 mm or less, flow regimes were found to be different from previous studies. Flow characteristics in these channels having a micro-gap (of 0.3 mm or less) are summarized as follows:

1. Even at very low air flow rates, bubbly flow was never observed.
2. At high liquid flow rates and low gas flow rates, because the small bubbles were squeezed and merged with each other, cap–bubbly flow existed in the channel. Generally, the shape of the cap-bubbles was a half circle at the top with a flat bottom. The distances of any two neighboring cap-bubbles were nearly the same.
3. At low gas flow rates and low liquid flow rates, slug–droplet flow existed in the 0.3 mm gap channel. The flow had the following characteristics: (1) the slug (also called "Taylor bubbles" in the literature) mainly contained a half circle head and a flat rectangular body. The slug was elongated and might cover over 50% of the channel length; (2) in the slug, isolated liquid droplets were adhered on the wall surface and were pushed by the slug. The droplets on the wall surface were dominated by the surface tension force, gravity and the drag force produced by the flowing slug; (3) between two slugs, isolated bubbles were never found. As mentioned above, the slug–droplet flow was quite different from the traditional slug flow performed in channels having a larger size gap (i.e. 1.0 mm and above).
4. At higher gas flow rates, churn flow existed in channels having a micro-gap. The slugs were more chaotic, frothy and distorted until they could not be discernible. The continuity of the liquid bridges was repeatedly destroyed due to the high local gas concentration in the liquid slug.
5. At much higher gas flow rates and low liquid flow rates, annular–droplet flow existed in the channel. The flow contained a continuous gas core and a surrounding liquid film. In the gas core, isolated liquid droplets were attached on the wall surface and were pushed by the flowing gas.

2. Experimental apparatus

A schematic diagram of the test loop is shown in Fig. 1. The water was provided by a pump and was regulated by a bypass line and the valves. The liquid flow entered the bottom plenum of the test section and mixed with air before entering the test section. The air/water mixture exited into the upper plenum and was separated in a separator collection tank. The air was

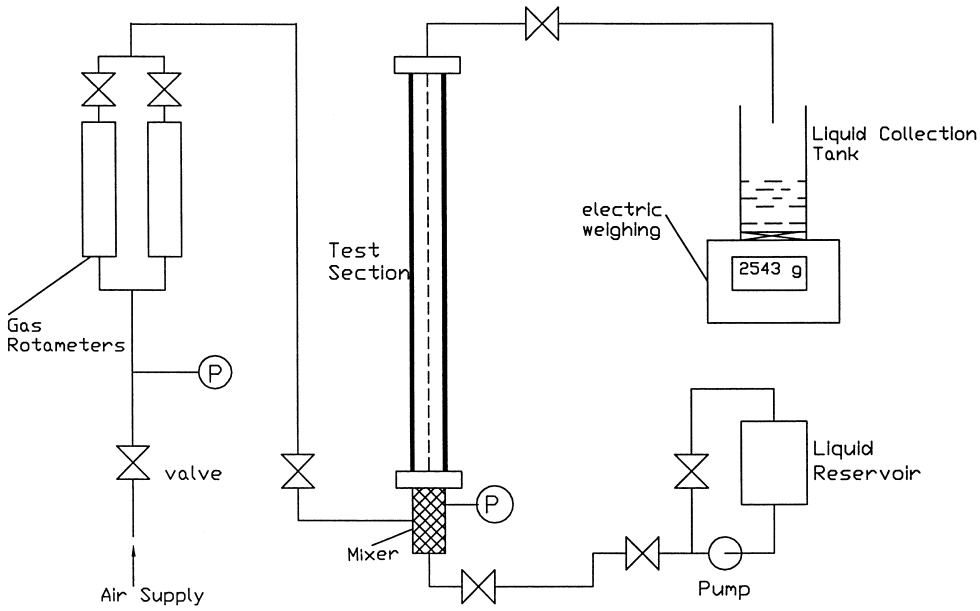

Fig. 1. Test loop of air/water system for flow regimes.

released into the atmosphere and the liquid was drained into the separator collection tank. By weighing the collection tank over a given period of time, the liquid flow rate could be accurately determined. The air was supplied by the laboratory air system and was controlled by gas rotameters.

Three rectangular test sections (260 mm in length and 12 mm in width) were made of Pyrex glass plate. Two pressure taps were separated by 220 mm, one located 20 mm after the entrance and another 20 mm before the exit of the test sections. The three test sections had different size gaps of 1.0, 0.6 and 0.3 mm. Measurements included the pressure before the fluids entering the test section and average liquid and gas flow rates. The visualization system, which is similar to the system used by Wilmarth and Ishii (1994), included a high speed camera and a monitor. The images were stored in the videotape for later analysing. Lighting was carefully adjusted to assure the clear identification of the gas–liquid interface. The shutter speed was chosen to be 1/4000 s.

3. Experimental results and discussion

3.1. Flow regimes in the channels having gap sizes of 1.0 and 0.6 mm

Even though considerable differences exist in the various researchers' definitions of two-phase flow patterns in channels having a larger size gap, it is generally agreed that flow regimes consist of bubbly flow, slug flow, churn flow and annular flow. Such typical flow regimes in these channels were schematically shown in Fig. 2 which includes two transition flows: cap–

bubbly transition flow [Fig. 2(b)] and slug–churn transition flow [Fig. 2(d)]. The description of classical two-phase flow regimes in vertical channels having a medium size gap is given by Collier (1981). Photographic observations of flow structures in the present vertical rectangular channels having mini-gaps of 0.6 and 1.0 mm confirmed such characteristics, except that the shape of gas bubbles in thin rectangular channels are two dimensional.

3.1.1. Bubbly flow

In bubbly flow, liquids are flowing in the channels as a continuous phase while gas is distributed in the continuous liquid phase as discrete small bubbles. In thin rectangular

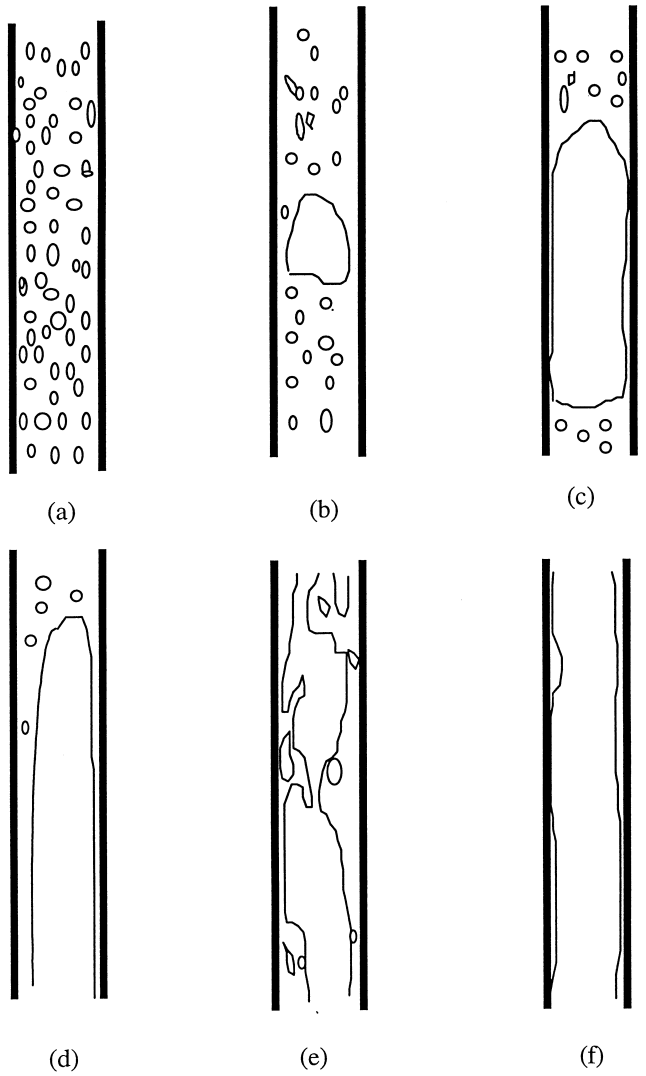

Fig. 2. Flow regimes in channels with medium size gaps: (a) bubbly flow; (b) cap–bubbly flow; (c) slug flow; (d) slug–churn flow; (e) churn–turbulent flow; (f) annular flow.

channels, the small bubbles are in the shape of two-dimensional circular cylinders, while in traditional circular channels of medium diameters, bubbles are spherical in shape.

3.1.2. Slug flow

Slug flow has large two-dimensional "Taylor bubbles" which contains an ellipsoidal nose and a flat rectangular body. The diameters of such Taylor bubbles approach the channel width, and the gas is separated from the side walls by slowly descending liquid films. The liquid flow is contained in liquid slugs which separate successive gas bubbles. Generally, the liquid bridges may contain small isolated gas bubbles.

3.1.3. Churn flow

Churn flow is formed by the breakdown of large gas bubbles in the slug flow. The gas flows in a more chaotic manner through the liquid which is mainly displaced to the channel wall. The flow has oscillatory or time varying characteristics.

3.1.4. Annular flow

In annular flow, a liquid film forms at the channel side wall with a continuous gas core. Large amplitude coherent waves are usually present on the surface of the film, and the continuous break up of these waves forms a source for small droplet entrainment which occurs in varying amounts in the central gas core.

Fig. 2(b) and (d) also shows two transition flows: the cap–bubbly transition flow and the slug–churn flow. The cap–bubbly flow is the transition from the bubbly flow to the slug flow, and the slug–churn flow is the transition from the slug flow to the churn flow. Usually, they do not contain particular regions in the flow regime map. Their characteristics are described by Wilmarth and Ishii (1994).

Figs. 3 and 4 are flow regime maps observed in the 12×1 mm and 12×0.6 mm vertical rectangular channels in the present study. Generally, flow regimes consist of bubbly flow, slug flow, churn flow and annular flow. The flow characteristics were not much different from those found in traditional channels having a large size gap except that the gas bubbles are two-dimensional in shape. However, a careful comparison between the present flow regime maps and flow regime maps for channels having a medium size gap found that the flow transition lines shifted sharply to the left for channels. With the size of the channel gap decreasing, transitions from bubbly flow to slug flow occurred at smaller gas flow rates because small bubbles were squeezed and merged with each other easily, thus the transition lines from bubbly flow to slug flow shifted to the left in the flow regime map, especially for the 0.6 mm gap vertical channel. Similarly, the transition line from slug flow to churn flow shifted to the left as the channel gap decreased. The reason mainly comes from the increased wall shear stress in rectangular channels having a mini-gap, which will be analyzed in later section in detail. The present flow regime map for the 12×1 mm vertical rectangular channel is similar to the flow regime map given by Wilmarth and Ishii (1994) for a 20×1 mm vertical rectangular channel. Mishima et al. (1993) developed a flow regime map for 40×1.07 mm vertical rectangular channels. For such a test section, no churn flow was observed. This may be due to the confusions between slug flow and churn flow, or churn flow and annular flow.

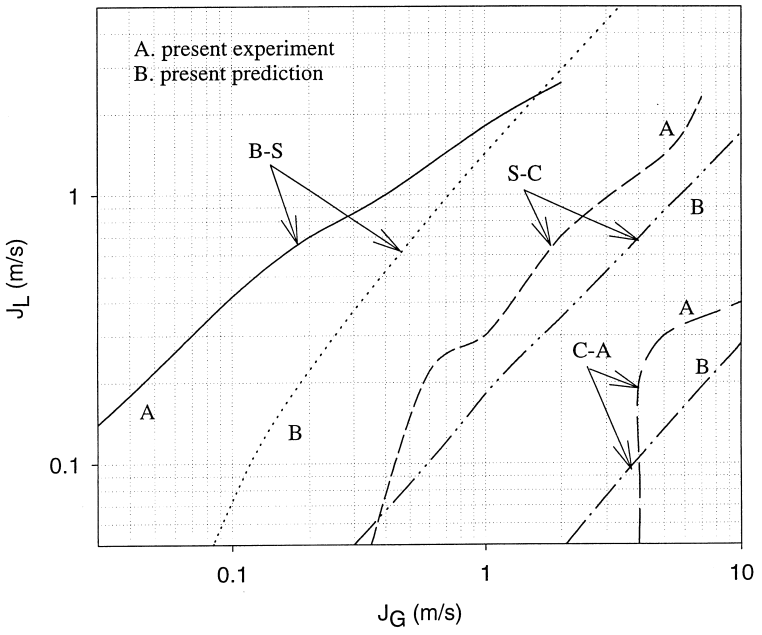

Fig. 3. Flow regime map in a vertical rectangular channel with $s = 1$ mm and $w = 12$ mm: B–S bubbly flow to slug flow transition; S–C slug flow to churn flow transition; C–A churn flow to annular flow transition.

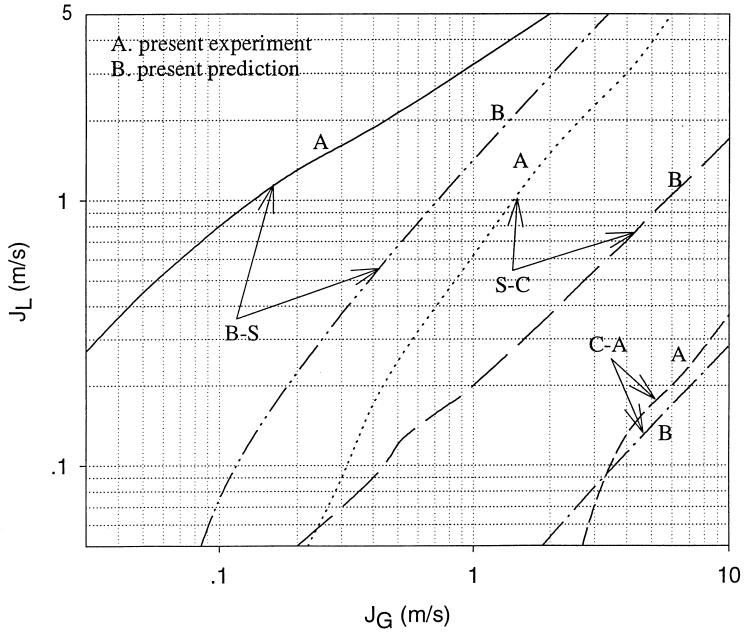

Fig. 4. Flow regime map in a vertical rectangular channel with $s = 0.6$ mm and $w = 12$ mm.

For the 12×1 mm channel, the present study showed that churn flow to annular flow transition occurs at about 4.0 m/s gas superficial velocity. The flow regime map given by Wilmarth and Ishii (1994) for a 20×1 mm channel showed that such transition occurs at about 5.0 m/s superficial gas velocity. However, early study for rectangular channels having a larger gap, e.g. Sadatomi and Sato (1982) showed that slug flow to annular flow transition occurs at superficial gas velocity larger than 10.0 m/s. This suggests that churn flow to annular flow transition, or slug flow to annular flow transition occur earlier with the decrease of the channel gap. This is also due to the increased interface shear stress and the increased wall shear stress.

3.2. Flow regimes in 0.3 mm gap vertical rectangular channel

As mentioned earlier, flow regimes in the present vertical rectangular channel having 0.3 mm micro-gap were quite different from the classical two-phase flow regimes found in channels having a larger gap. The present paper found two important phenomena: (1) bubbly flow, which existed in channels having larger gaps as shown in Fig. 2(a) was never observed in the 0.3 mm gap rectangular channel; (2) at smaller liquid flow rates, liquid droplets were observed to be attached to the wall surface and were pushed by the gas phase. Therefore, we now define two new flow regimes: slug–droplet flow and annular–droplet flow. Typical photographs of four different flow structures are shown in Fig. 5 with the corresponding flow regimes shown in Fig. 6. The four flow regimes: cap–bubbly flow, slug–droplet flow, churn flow and annular–droplet flow, are described in the following.

3.2.1. Cap–bubbly flow

Even at very low gas flow rates, no bubbly flow (which is shown in Fig. 2(a) in rectangular channels having gaps of 0.6, 1.0 mm or larger), was observed in the 0.3 mm gap channel. This is to say that bubbly flow was suppressed in channels having a mini gap. In micro-gap channels, small isolated bubbles were squeezed and merged with each other easily. Such an effect caused the coalescence of small bubbles to form cap–bubbly flow. The cap–bubbly flow can occur stably in the channel at high liquid flow rates and low gas flow rates (represented in the upper-left region in Fig. 6). The shape of the cap-bubble was a two-dimensional half circle at the top with a flat bottom. The diameter of such a cap-bubble may approach the width of the channel. The distances between the two neighboring cap-bubbles were nearly the same. At cap–bubbly flow condition, a continuous increase in the gas flow rate can lead to churn flow while a continuous decrease in the liquid flow rate can cause slug–droplet flow.

3.2.2. Slug–droplet flow

At low gas flow rates and low liquid flow rates, there existed slug–droplet flow in the 0.3 mm gap vertical rectangular channel. Compared with the classical slug flow carried out in channels having a large gap, slug–droplet flow had the following special characteristics: (1) in the elongated slug, liquid droplets were always observed. Due to the small confined gap of the channel, isolated liquid droplets were adhered to the wall surface and were pushed by the flowing slug. The droplets on the wall surface were under the influence of the surface tension,

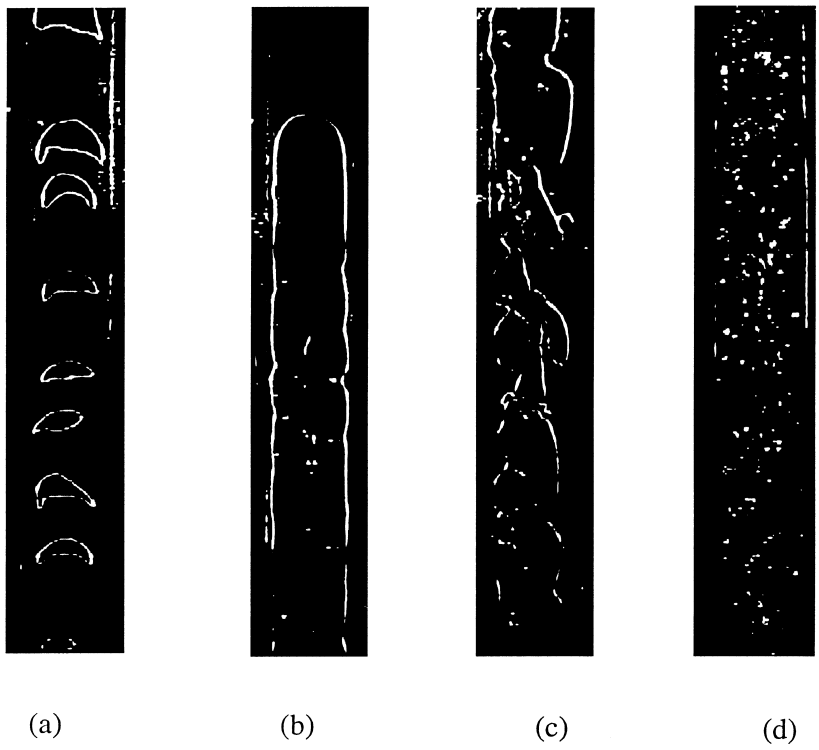

Fig. 5. Typical flow regime in a 0.3 mm vertical rectangular channel: (a) cap–bubbly flow; (b) slug–droplet flow; (c) churn flow; and (d) annular–droplet flow.

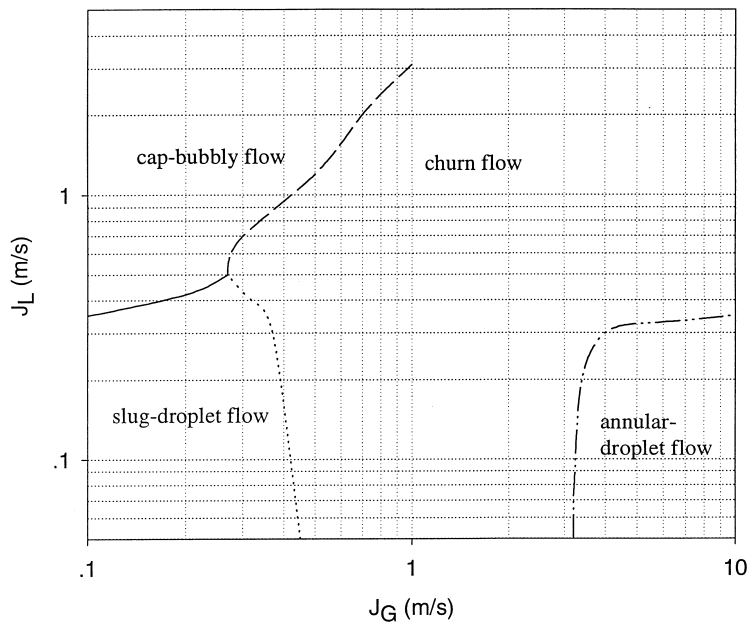

Fig. 6. Flow regime map in a vertical channel with $s = 0.3$ mm, and $w = 12$ mm.

gravity and drag force created by the gas phase; (2) the liquid bridges which separated successive slugs, did not contain any small gas bubbles.

In the present 0.3 mm gap channel, slug–droplet flow occurred only at low gas flow rates and low liquid flow rates. Early studies showed that classical slug flow can cover a wide range of liquid flow rates at medium gas flow rates. The transition from slug–droplet flow to churn flow in the 0.3 mm gap channel was found to occur at nearly 0.46 m/s gas superficial velocity.

3.2.3. Churn flow

Churn flow in the 0.3 mm gap vertical rectangular channel was similar to that found in channels having a large gap. The characteristics were described in the above section. Churn flow covered a large range of liquid flow rates at medium gas superficial velocity.

3.2.4. Annular–droplet flow

At the churn flow condition, continued increase in the gas flow rate will lead to an annular–droplet flow. Such transition occurred at about 3.3 m/s gas superficial velocity. But annular–droplet flow existed only at liquid superficial velocities below 0.34 m/s. Annular–droplet flow consisted of a continuous gas core and a surrounding liquid film which separated the gas core and the side walls of the channel. Compared with the classical annular flow in channels having a large gap, annular–droplet flow contained isolated liquid droplets in the gas core. The liquid droplets were attached on the wall surface and were pushed by the gas core. Such characteristics were similar to slug–droplet flow in mini-gap channels as discussed earlier.

4. Flow regime transition criteria in rectangular channel

This section presents an analysis of the criteria for flow regime transitions from bubbly flow to slug flow, slug flow to churn flow and the formation of annular flow, A new model to derive the transition criteria for the formation of annular flow will be presented. Special attention will be paid to analysing the force balance of the gas core and the liquid film.

4.1. Bubbly flow to slug flow transition

In a bubbly flow there is a finite probability that, because of their random motion, individual bubbles will collide and coalesce to form large bubbles. For void fraction α below about 0.1 the collision frequency would be low (Mishima and Ishii, 1984). Above this value the frequency rose steeply until at $\alpha_{cr} = 0.3$ a slug flow formed which was to be expected (Mishima and Ishii, 1984).

We used the following relationship between J_G and J_L, which is derived from the drift velocity for bubbly flow.

$$v_G = \frac{J_G}{\alpha} = C_o(J_G + J_L) + v_b. \tag{1}$$

Where J_G and J_L are the superficial velocities of gas and liquid, respectively, C_o is the distribution parameter and v_b the bubble rising velocity relative to the liquid phase. Sadatomi

and Sato (1982) suggested that for a medium size rectangular channel, v_b could be well correlated by

$$v_b = 0.35\sqrt{gD_e} \tag{2}$$

where g is the gravity, D_e is the equi-periphery diameter, and can be written as

$$D_e = 2(s + w)/\pi \tag{3}$$

where s and w are the channel gap and width.

Combining Eqs. (1)–(3), we obtain the following criterion for bubbly flow to slug flow transition:

$$J_L = \left(\frac{1}{\alpha_{cr}C_o} - 1\right)J_G - \frac{0.35\sqrt{gD_e}}{C_o} \tag{4}$$

where C_o is given by

$$C_o = 1.35 - 0.35\sqrt{\frac{\rho_G}{\rho_L}} \tag{5}$$

for rectangular channels. ρ_G and ρ_L are the densities of gas and liquid, respectively.

4.2. Slug flow to churn flow transition

The concept of transition from slug flow to churn flow was mainly based on Mishima and Ishii (1984). The transition occurs when the mean void fraction over the entire region exceeds that over the slug bubble section. When the transition begins, the two neighboring slug bubbles start to touch each other, and the flow becomes unstable. Mishima and Ishii (1984) obtained the slug bubble mean void fraction α_m based on the potential flow analysis. The local axial void fraction $\alpha(h)$ at the distance h from the slug nose is (Mishima and Ishii, 1984)

$$\alpha(h) = \frac{\sqrt{2gh\Delta\rho/\rho_L}}{\sqrt{2gh\Delta\rho/\rho_L} + (C_o - 1)(J_G + J_L) + v_b}. \tag{6}$$

The mean void fraction is given by

$$\alpha_m = \frac{1}{L_b}\int_0^{L_b} \alpha(h)\,dh \tag{7}$$

where L_b is the slug bubble length, $\Delta\rho$ is the density difference between the two phases. Substituting Eq. (6) into Eq. (7) and performing the integration yields

$$\alpha_m = 1 - 2X + 2X^2 \ln\left(1 + \frac{1}{X}\right) \tag{8}$$

where

$$X = \sqrt{\frac{\rho_L}{2g\Delta\rho L_b}}\left[(C_o - 1)(J_G + J_L) + 0.35\sqrt{gD_e}\right]. \tag{9}$$

Mishima and Ishii (1984) found that Eq. (8) can be represented by the following equation

$$\alpha_m = 1 - 0.813X^{0.75}. \tag{10}$$

We now estimate the slug bubble length L_b in Eq. (7). Somewhere below the nose of a slug bubble, the gravity force on the liquid film is balanced by the wall shear stress and the flow becomes fully developed. Applying the force balance on the liquid film around the slug gives

$$\frac{f}{2}\rho_L v_{fsb}^2 2(s + w) = \Delta\rho g A(1 - \alpha_{sb}) \tag{11}$$

where v_{fsb} is the terminal film velocity in the bubble slug section, α_{sb} is the void fraction corresponding to the terminal film velocity v_{fsb}, A is the channel cross section area, and f is the wall friction factor which can be estimated as

$$f = C_f\left[\frac{(1 - \alpha_{sb})v_{fsb}D_h}{v_L}\right]^{-m} \tag{12}$$

with $m = 1$ for laminar flow and $m = 0.25$ for turbulent flow. D_h and v_L are the channel hydraulic diameter and the liquid viscosity. C_f is dependent on the Reynolds number defined as

$$Re = \frac{(1 - \alpha_{sb})v_{fsb}D_h}{v_L}. \tag{13}$$

For laminar flow in rectangular channels, Cornish (1982) gives

$$C_{fl} = \frac{24}{(\Omega + 1)^2}\left(1 - \frac{192\Omega}{\pi^5}\sum_{n=1}^{\infty}\frac{\tanh\left(\frac{(2n-1)\pi}{2\Omega}\right)}{(2n-1)^5}\right)^{-1} \tag{14}$$

where $\Omega = s/w$ is the aspect ratio.

For the turbulent friction factor of single phase flow in a non-circular channel, Sadatomi et al. (1982) took account of channel geometry and proposed the following empirical relationship between the laminar coefficients C_{fl}, which is given by Eq. (14), and the turbulent coefficient C_{ft}:

$$\frac{C_{ft}}{C_{ft,tube}} = \left(0.0154\frac{C_{ft}}{C_{fl,tube}} - 0.012\right)^{1/3} + 0.85 \tag{15}$$

where $C_{ft,tube} = 0.0791$ is the turbulent coefficient in tubes. C_{fl} is given by Eq. (14) for a rectangular channel. $C_{fl,tube} = 16$ is the laminar coefficient in tubes.

Substituting the following basic relationship of a two-phase mixture (Mishima and Ishii, 1984)

$$v_{\mathrm{fsb}} = \frac{\alpha_{\mathrm{sb}} v_{\mathrm{G}} - (J_{\mathrm{G}} + J_{\mathrm{L}})}{1 - \alpha_{\mathrm{sb}}} \tag{16}$$

into Eq. (11) and solving for α_{sb} gives

$$\alpha_{\mathrm{sb}} = \frac{J_{\mathrm{G}} + J_{\mathrm{L}} + (1 - \alpha_{\mathrm{sb}})^{3/(2-m)} \left[2C_{\mathrm{f}} \left(\frac{D_{\mathrm{h}}}{v_{\mathrm{L}}} \right)^{-m} \frac{\rho_{\mathrm{L}}}{\Delta\rho g D_{\mathrm{h}}} \right]^{1/(m-2)}}{C_{\mathrm{o}}(J_{\mathrm{G}} + J_{\mathrm{L}}) + v_{\mathrm{b}}}. \tag{17}$$

On the other hand, we obtain $\alpha(L_{\mathrm{b}})$ from Eq. (6) as

$$\alpha(L_{\mathrm{b}}) = \frac{\sqrt{2gL_{\mathrm{b}}\Delta\rho/\rho_{\mathrm{L}}}}{\sqrt{2gL_{\mathrm{b}}\Delta\rho/\rho_{\mathrm{L}}} + (c_{\mathrm{o}} - 1)(J_{\mathrm{G}} + J_{\mathrm{L}}) + v_{\mathrm{b}}}. \tag{18}$$

Comparing Eq. (9) and Eq. (18), we obtain

$$X = \frac{1 - \alpha(L_{\mathrm{b}})}{\alpha(L_{\mathrm{b}})}. \tag{19}$$

Physically $\alpha(L_{\mathrm{b}}) = \alpha_{\mathrm{sb}}$ which is given by Eq. (17). Replacing $\alpha(L_{\mathrm{b}})$ by α_{sb} in Eq. (19) gives X. Substituting X into Eq. (10) gives the mean void fraction α_{m}. When $\alpha \geq \alpha_{\mathrm{m}}$ is satisfied, the transition from slug flow to churn flow is postulated to occur, where α is given by

$$\alpha = \frac{J_{\mathrm{G}}}{C_{\mathrm{o}}(J_{\mathrm{G}} + J_{\mathrm{L}}) + v_{\mathrm{b}}}. \tag{20}$$

4.3. Formation of annular flow

When the gas flow rate is high enough, the transition from slug flow to annular flow, or churn flow to annular flow occurs. In a fully developed annular flow, most liquids are flowing upwards along the channel wall. However, some liquid droplets may be entrained in the gas core. Waves can be created in the interface of the gas core and the liquid film. Taitel et al. (1980) considered that annular flow was formed when the gas velocity was high enough to entrain and push liquid droplets in the gas core. Using the force balance between the liquid gravity and the drag force created by the gas phase, they developed the following criteria (Taitel, 1980):

$$\frac{J_{\mathrm{G}} \rho_{\mathrm{G}}^{0.5}}{\left[\sigma g(\rho_{\mathrm{L}} - \rho_{\mathrm{G}})\right]^{0.25}} = 3.0 \tag{21}$$

where σ is the surface tension. Eq. (21) shows that the transition criterion depends only on the gas superficial velocity and the fluid properties. However, as mentioned in Section 3.1, with channel size decreasing, the air superficial velocity at which annular flow forms, decreases. This means that channel geometry affects the formation of annular flow. In addition, liquid superficial velocity was another important parameter which affects the annular flow. This led

us to develop another relationship which will take into consideration the channel geometry to predict the flow regime transition.

Based on the experimental data with two-phase mixture flowing in tubes, Armand (1983) found that when the volumetric quality β is less than 0.9, there exists the following linear relationship between the void fraction α and volumetric quality β:

$$\alpha = 0.833\beta. \tag{22}$$

When β is larger than 0.9, void fraction α is increased sharply. Such phenomenon means that the relationship between α and β is nearly the same for bubbly flow, slug flow or churn flow. But if annular flow is formed, the void fraction α is sharply increased due to the continuous gas phase existing in the channel. Thus, it will now be assumed that $\alpha = 0.833 \times 0.9 = 0.75$ when annular flow is formed.

Applying the force balance for gas core and the liquid film, we obtain

$$-A_G \frac{dP}{dz} - \tau_i S_i - A_G \rho_G g = 0, \tag{23}$$

$$-A_L \frac{dP}{dz} - \tau_w S_w + \tau_i S_i - A_L \rho_L g = 0, \tag{24}$$

where τ_i is the interface shear stress, τ_w is the wall shear stress, $S_i = 2(s + w)\alpha^{0.5}$ is the interfacial periphery and $S_w = 2(s + w)$ is the wall periphery. A_L and A_G are flow cross section areas of the liquid phase and the gas phase, respectively. dP/dz is the pressure gradient along the flow direction.

Eliminating dP/dz between Eq. (23) and Eq. (24) and substituting the following expressions

$$A_L = A(1 - \alpha), \tag{25}$$

$$A_G = A\alpha \tag{26}$$

into Eq. (23) and Eq. (24) gives

$$\frac{\tau_i S_i}{A}\left(\frac{1}{\alpha} + \frac{1}{1-\alpha}\right) - (\rho_L - \rho_G)g - \frac{4\tau_w}{D_h(1-\alpha)} = 0 \tag{27}$$

and

$$\tau_i = f_i \frac{\rho_G}{2}(v_G - v_L)^2. \tag{28}$$

Govan et al. (1989) suggested the following relationships to calculate the interface friction coefficient

$$f_i = C_G\left(\frac{D_h J_G}{v_G}\right)^{-n_1}\left[1 + 6(1-\alpha)\left(\frac{\rho_L}{\rho_G}\right)^{1/3}\right] \tag{29}$$

where v_G is the gas viscosity. Substituting Eq. (29) into Eq. (28) and using $v_G = J_G/\alpha$ and $v_L = J_L/1 - \alpha$ gives

$$\tau_i = C_G\left(\frac{D_h J_G}{v_G}\right)^{-n_1}\left[1+6(1-\alpha)\left(\frac{\rho_L}{\rho_G}\right)^{1/3}\right]\frac{1}{2}\rho_G\left(\frac{J_G}{\alpha}-\frac{J_L}{1-\alpha}\right)^2. \tag{30}$$

The wall friction shear stress is given by

$$\tau_w = C_L\left(\frac{v_L D_L}{v_L}\right)^{-n_2}\frac{1}{2}\rho_L v_L^2 \tag{31}$$

where D_L is the hydraulic diameter of the liquid phase, and

$$v_L = \frac{J_L}{1-\alpha}, \tag{32}$$

$$D_L = D_h(1-\alpha). \tag{33}$$

Substituting Eqs. (32) and (33) into Eq. (31) gives

$$\tau_w = C_L\left(\frac{J_L D_h}{v_L}\right)^{-n_2}\frac{1}{2}\rho_L\left(\frac{J_L}{1-\alpha}\right)^2. \tag{34}$$

Combining Eqs. (27), (30) and (34), and using $\alpha = 0.75$, the following transition criteria was obtained

$$1.33J_G - 4J_L = \sqrt{\frac{(\rho_L-\rho_G)gD_h + 128C_L\left(\frac{J_L D_h}{v_L}\right)^{-n_2}\rho_L J_L^2}{9.24C_G\left(\frac{D_h}{v_G}\right)^{-n_1}\rho_G\left[1+1.5\left(\frac{\rho_L}{\rho_G}\right)^{1/3}\right]}}J_G^{n_1/2} \tag{35}$$

In Eq. (35), C_L and C_G are dependent on the Reynolds number defined as $D_h J_G/v_G$ and $D_h J_L/v_L$. The determination of C_L and C_G are similar to that of C_f as discussed in Section 4.2. For a laminar flow, n_1 or n_2 is equal to unity; for a turbulent flow, n_1 or n_2 is equal to 0.25.

5. Comparisons of present prediction with experimental data

Mishima et al. (1993) developed flow regime maps for a rectangular channel, 200 cm in length and 40 mm in width, having gaps of 1.07, 2.45 and 5.0 mm. Flow regime maps for a channel gap of 1.07 mm is shown in Fig. 7. It is seen that the experimental transition line of bubbly flow to slug flow only shifted slightly to the left compared with the present prediction line. Mishima et al. (1993) did not find churn flow in such a test section. Fig. 8 shows the flow regime maps for a vertical channel having 2.45 mm gap. Good agreements were obtained between data of Mishima et al. (1993) (curves marked by A) and the present predictions (curved marked by B) except that the annular flow observed from experiments was formed at a lower value of J_G than that by predictions.

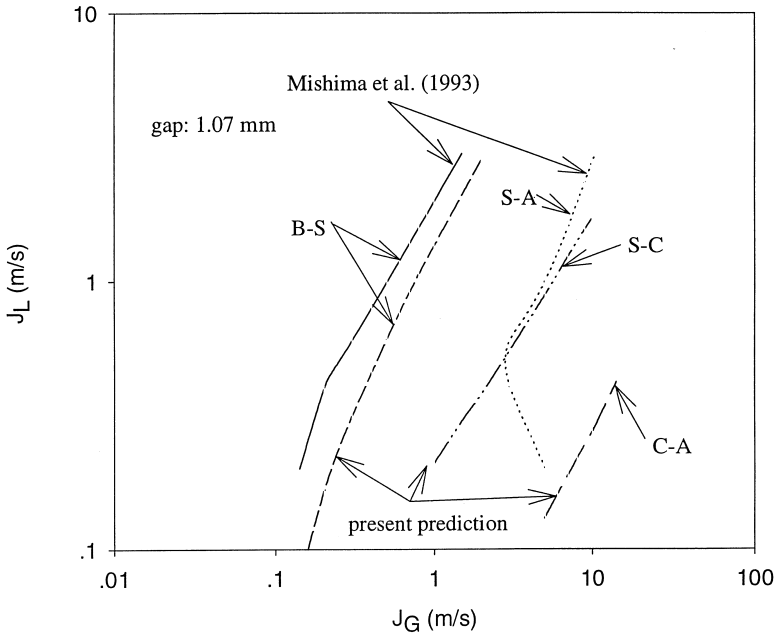

Fig. 7. Flow regime comparison with the present prediction for a 1.07 mm gap vertical channel flow: B–S bubbly flow to slug flow transition; S–A slug flow to annular flow transition; S–C slug flow to churn flow transition; C–A churn flow to annular flow transition.

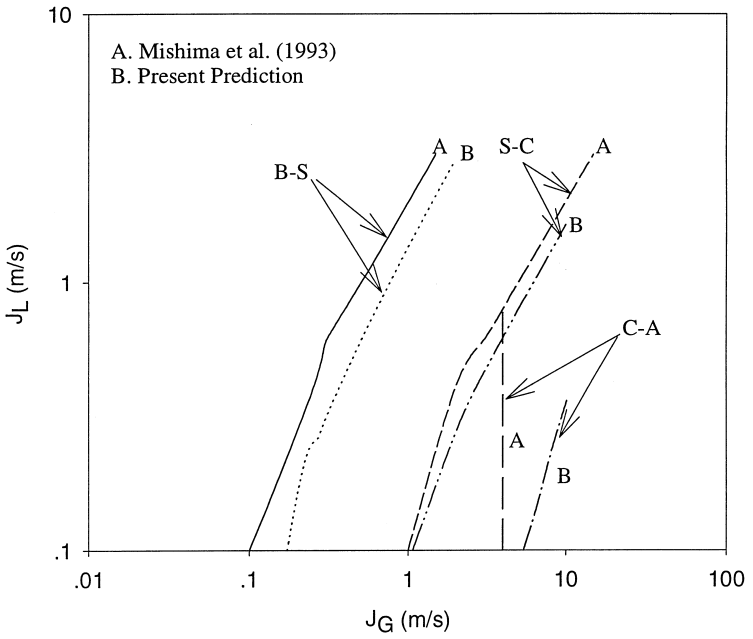

Fig. 8. Flow regime transition comparison with the present prediction for a 2.4 mm gap vertical channel flow; B–S bubbly flow to slug flow transition; S–C slug flow to churn flow transition; C–A churn flow to annular flow transition.

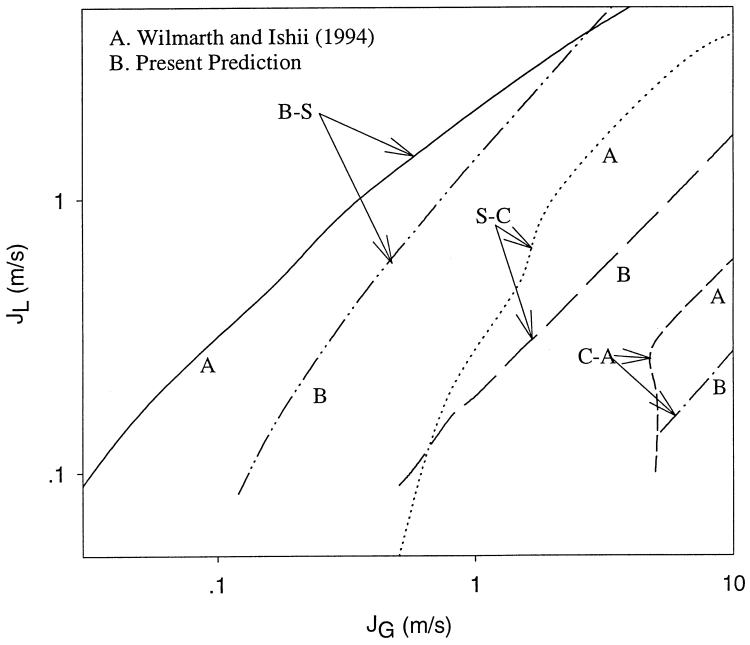

Fig. 9. Flow regime transition comparison with the present prediction for a 1 mm gap vertical channel flow: B–S bubbly flow to slug flow transition; S–C slug flow to churn flow transition; C–A churn flow to annular flow transition.

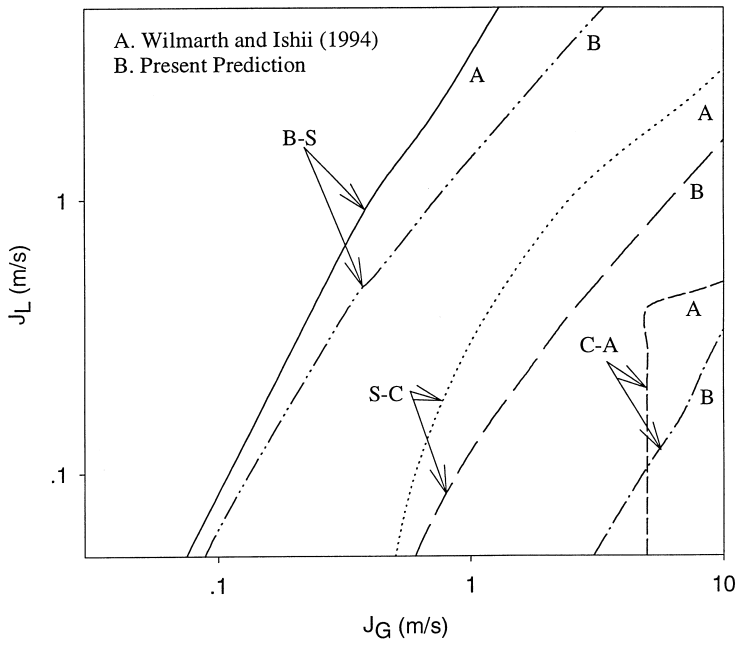

Fig. 10. Flow regime transition comparison with the present prediction for a 2 mm gap vertical channel flow: B–S bubbly flow to slug flow transition; S–C slug flow to churn flow transition; C–A churn flow to annular flow transition.

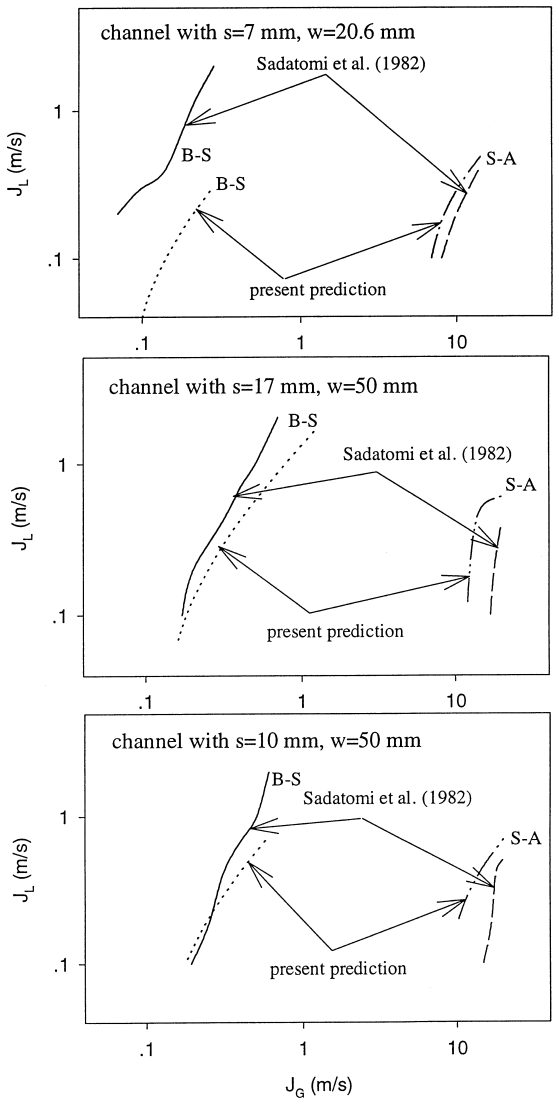

Fig. 11. Flow regime comparison with present prediction in medium size rectangular channels with a medium size gap.

Wilmarth and Ishii (1984) obtained the flow regime maps for 20×1 mm and 15×2 mm vertical rectangular channels. Their results are shown in Figs. 9 and 10. Also shown in these figures are the present prediction lines. In these two figures, reasonably good agreement was obtained for annular flow. For transitions from bubbly flow to slug flow and from slug flow to churn flow, the transition lines given by the experimental data of Wilmarth and Ishii (1994) shifted to the left of the theoretical prediction. For the rectangular channel having a mini size gap, the transition from bubbly flow to slug flow may occur earlier because the small bubbles were squeezed and merged with each other in the channel.

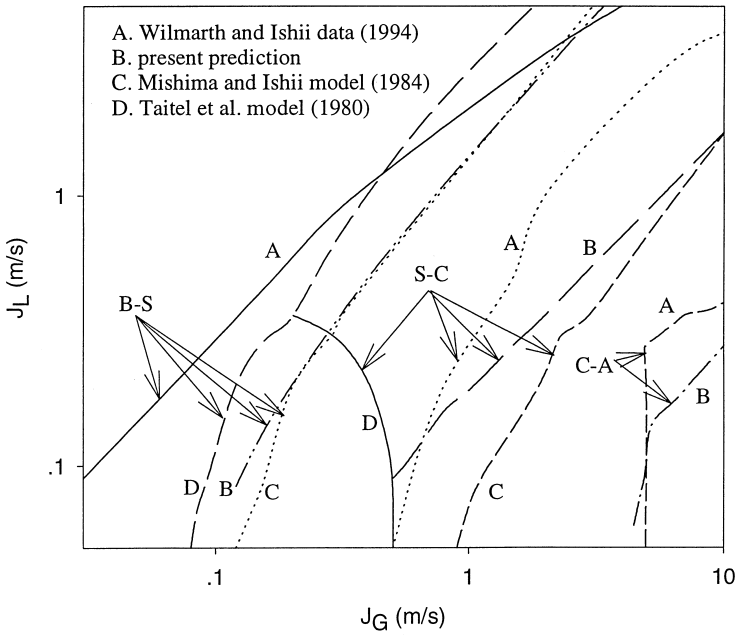

Fig. 12. Flow regime transition comparison with different theories for a vertical rectangular channel with $s = 1$ mm and $w = 20$ mm: B–S bubbly flow to slug flow transition; S–C slug flow to churn flow transition; C–A churn flow to annular flow transition.

Figs. 3 and 4 show the comparison of transition lines between our experimental results and our predictions. Flow regimes in our 12×1 mm channel were similar to those performed with a 20×1 mm channel by Wilmarth and Ishii (1994) because only slightly different geometries were used. For the present rectangular channels having mini gaps, the present prediction results were less satisfactory except for annular flow. With channel gap decreasing, the experimental transition lines shifted to the left, and bubbly flow only covered a small region. For the 0.3 mm micro gap channel, flow regimes were quite different from the classical flow regimes performed in channels having a medium size gap. Some different characteristics were found, and the present transition criteria could not predict such transitions.

Fig. 11 shows a comparison of transition lines between the present theory and experimental data of Sadatomi et al. (1982) for three rectangular channels having gap sizes of 7, 10 and 17 mm. In such channels, only bubbly flow, slug flow and annular flow were found. Our predictions matched with their experimental data quite well, except that large differences were found between predictions and experiment for bubbly flow to slug flow transition in a 20.6×7 mm channel.

Finally, comparisons will be made among different transition criteria with the experiments by Wilmarth and Ishii (1994). Fig. 12 shows such a comparison. For bubbly flow to slug flow transition, Taitel et al. (1980) predicted the B–S transition line reasonably well. However, Taitel et al. (1980) could not predict the transition from slug flow to churn flow well. Predicted transition lines by Mishima and Ishii (1984) shifted to the right compared with the

experimental data. As mentioned above, these two models cannot predict annular flow well because they do not take into consideration the channel geometry effect.

The present model predicted annular flow quite well. This is mainly because our annular flow criteria take into consideration the increased wall shear stress and interface shear stress. From bubbly flow to slug flow and from slug flow to churn flow, the present predicted transition lines are closer to the experimental data than those given by Mishima and Ishii (1984), especially for slug flow to churn flow transition. This is because the present predictions take into consideration the increased wall shear stress in small gap rectangular channels.

6. Summary and conclusions

1. A study of two-phase flow regimes in rectangular channels having narrow gaps has been performed. The three test sections are 260 mm in length and 12 mm in width with different gaps of 1.0, 0.6 and 0.3 mm. Flow regimes were observed by a CCD camera and were identified by examining the video images.
2. Flow regimes for 1.0 and 0.6 mm channel gaps found to be similar to those in channels having a larger gap, which mainly consist of bubbly flow, slug flow, churn flow and annular flow. However, in rectangular channels having mini gaps, bubbles are flattened and two-dimensional in shape.
3. In channels having a mini-gap, the transition lines from bubbly flow to slug flow, from slug flow to churn flow, and from churn flow to annular flow shifted to the left in a flow regime map. Especially for a 0.6 mm gap channel, bubbly flow covered a relatively small region. This is because small bubbles were squeezed in the gap and merged with each other. The reason that the transition line from slug flow to churn flow shifted to the left is mainly because of the increased friction shear stress. Annular flow is formed at lower gas velocities. This is also due to the increased wall shear stress and increased interface shear stress.
4. In the channel having a micro-gap of 0.3 mm, flow structures were different from the classical flow structures in channels having a large size gap or in channels having 1.0 and 0.6 mm gaps. Two important phenomena were: bubbly flow was never observed; at low liquid flow rates, liquid droplets were always attached on the wall surface and were pushed by the gas phase. Based on the experimental observation, the present investigation found two new flow regimes: slug–droplet flow and annular–droplet flow. Thus, flow regimes in channels having a micro-gap consist of cap–bubbly flow, slug–droplet flow, churn flow and annular–droplet flow. The flow characteristics have been described in detail in the present paper.
5. This paper modeled the transition from bubbly flow to slug flow at a void fraction at 0.3 using the bubble rising velocity for rectangular channels. The paper extended the Mishima and Ishii (1984) model to predict the transition from slug flow to churn flow, with particular attention to the increased shear stress in the rectangular channels. For annular flow, the present paper specified that annular flow was formed at a critical void fraction of 0.75. Applying the force balances on the gas core and the liquid film, a new criterion was

developed. Particular attention was also given to the increased interface shear stress and wall shear stress.

6. For rectangular channels having a mini size gap, our predictions matched the experiment data well. The present predictions agreed with the experimental data of Mishima et al. (1993) reasonably well. When compared with the Wilmarth and Ishii (1994) experimental data, the predicted transition lines shifted to the right. However, our predictions are closer to the experimental transition lines than those by Mishima and Ishii (1984). For most conditions, the predictions matched the experimental data well for annular flow. The above improvements mainly came from applying the increased friction coefficient for rectangular channels.
7. The present predictions did not agree with the present 0.6 mm gap channel data well. For such channels, bubbly flow only occurred in a small region in the flow regime map. For channels having a 0.3 mm or micro-gap, a new theory must be developed because some new flow characteristics begin to appear.

Acknowledgements

This work was supported by a Hong Kong RGC Earmarked Research Grant No. HKUST 6045/97E.

References

Armand, A.A., 1946. The resistance during the movement of a two-phase system in horizontal pipes. Izvestia Vses. Teplo. Inst. 1, 16–23.

Bowers, M.B., Mudawar, I., 1994. High flux boiling in low flow rate, low pressure drop mini-channel and micro-channel heat sinks. Int. J. Heat Mass Transfer 37 (2), 321–332.

Collier, J.G., Thome, J.R., 1994. Convective Boiling and Condensation. 3rd. McGraw-Hill, New York.

Cornish, R.J., 1928. Flow in a pipe of rectangular cross-section. Proc. of Royal Society of London, series A 120, 691–700.

Govan, A.H., Hewitt, G.F., Owen, D.G., Burnett, G., 1989. Wall shear stress measurements in vertical air-water annular two-phase flow. Int. J. Multiphase Flow 15, 307–325.

Mishima, K., Ishii, M., 1984. Flow regime transition criteria for upward two-phase flow in vertical tubes. Int. J. Heat Mass Transfer 27, 723–737.

Mishima, K., Hibiki, T., Nishihara, H., 1993. Some characteristics of gas–liquid flow in narrow rectangular ducts. Int. J. Multiphase Flow 19, 115–124.

Peng, X.F., Peterson, G.P., 1996. Convective heat transfer and flow friction for water flow in microchannel structures. Int. J. Heat Mass Transfer 39, 2599–2608.

Peng, X.F., Wang, B.X., 1993. Forced convection and flow boiling heat transfer for liquid flowing through micro-channels. Int. J. Heat Mass Transfer 36, 3421–3427.

Peng, X.F., Wang, B.X., Peterson, G.P., Ma, H.B., 1995. Experimental investigation of heat transfer in flat plates with rectangular micro-channels. Int. J. Heat Mass Transfer 38, 127–137.

Sadatomi, Y., Sato, Y., Saruwatari, S., 1982. Two-phase flow in vertical noncircular channels. Int. J. Multiphase Flow 8, 641–655.

Taitel, Y., Bornea, D., Dukler, A.E., 1980. Modeling flow pattern transitions for steady upward gas–liquid flow in vertical tubes. AIChE J. 26, 345–354.

Troniewski, L., Ulbrich, R., 1984. Two-phase gas–liquid flow in rectangular channels. Chem. Engng Science 39, 751–765.

Wilmarth, T., Ishii, M., 1994. Two-phase flow regimes in narrow rectangular vertical and horizontal channels. Int. J. Heat Mass Transfer 37, 1749–1758.

Yao, S.C., Chang, Y., 1983. Pool boiling heat transfer in a confined space. Int. J. Heat Mass Transfer 26, 841–848.